
Quality Technology & Quantitative Management
Vol. 9, No. 1, pp. 59-77, 2012

QTQM

A Statistical Method for Crack Detection from Vibrothermography Inspection Data

Chunwang Gao and William Q. Meeker

Department of Statistics, Center for Nondestructive Evaluation, Iowa State University, Ames, IA, USA
(*Received* October 2010, *accepted* March 2011)

Abstract: Nondestructive evaluation methods are widely used in quality control processes for critical components in systems such as aircraft engines and nuclear power plants. These same methods are also used in periodic field inspection to assure that the system continues to be reliable while it is in service. This paper describes a detection algorithm to automatically analyze vibrothermography sequence-of-image inspection data used to detect cracks in jet engine fan blades. Principal components analysis is used for dimension reduction. Then the fitted coefficients of the first principal component are processed by using robust regression to produce studentized residuals that are used in the crack-detection rules. We also show how to quantify the probability of detection for the algorithm. The detection algorithm is both computationally efficient and accurate. It correctly identified several cracks in our experimental data that were not detected by the standard human visual inspection method.

Keywords: Image analysis, nondestructive evaluation, POD, sonic IR, thermosonics.

1. Introduction

1.1. Vibrothermography in Nondestructive Evaluation

Vibrothermography, also known as Sonic Infrared (IR), thermoacoustics and thermosonics, is described, for example, in Henneke and Jones [2], Reifsnider *et al.* [9] and recent work by Holland [3]. It is a technique used for detecting cracks in industrial, dental, and aerospace applications. A pulse of sonic or ultrasonic energy is applied to a unit to make the unit vibrate. If a crack exists in the unit, it is expected that the faces of the crack will rub against each other, resulting in a temperature increase near the crack. An infrared camera is used to measure the temperature change in a sequence of frames over time, which we refer to as a movie. In this paper, we present methods for studying and analyzing the movie data for purposes of crack detection.

1.2. Purpose of the Study

In this paper, we develop a systematic method to automatically analyze the data generated in vibrothermography inspections. The goal is to have a screening algorithm that can detect the possible presence of cracks in a movie, so that experienced evaluators only need to evaluate movies for which identification is uncertain.

2. Experimental Data

The vibrothermography data provided to us consisted of a movie for each of 70 specimens (60 with cracks and 10 blanks with no crack). For each movie, we were also given information on the size of the crack and whether an inspector had been able to detect the crack or not from watching an enhanced version of the movie (background of an early image

subtracted out).

2.1. Crack Signal Signature

There were either 31 or 55 frames, ordered in time, in each of the movies that we received. Each frame contains 256 by 256 pixels. Each pixel is represented by a 12-bit integer. Figure 1 shows four frames (the 4th, 10th, 20th, and 30th) in Movie 02. Movie 02 has a strong signal near its center. The 4th frame shows no sign of a signal. The signal is clearly visible by the 10th frame and the signal size (the dot size) continues to grow until the last frame in the movie.

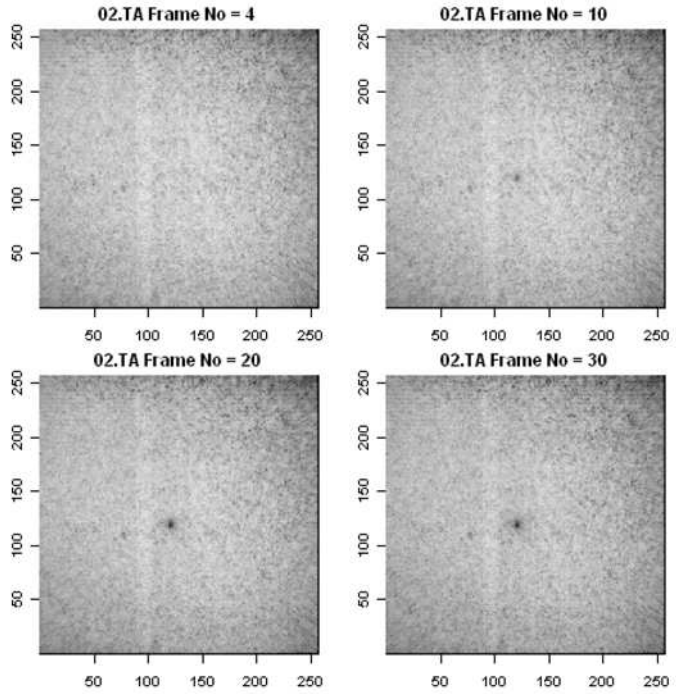

Figure 1. Frames (4th, 10th, 20th and 30th) from Movie 02, which has a strong crack signal around the center. The four frames show the strength of the crack signal grows with time.

Figure 2 shows the temporal behavior of a grid of $3 \times 3 = 9$ pixels approximately centered on a crack signal. The paths with stronger signals are closer to the center of the square and those with weaker signals are near the corners (maximum distance from the center). The thick dark line on the top is the signal strength at the center of the 3×3 matrix. The legend in the north-west corner gives idea of which line corresponds to which point in the movie. For example, the "+" is the south-east center of 9 pixels.

Figure 3 illustrates the intensity change in the Y direction at Frame 30, which is near the end of the energy input. A very similar shape appears in the X direction. The plots show that the crack signal has a width of around 14 pixels (which is the windows size used in the scan calculation), and that the increase is almost linear from the edge of the crack signal to the center of the crack signal.

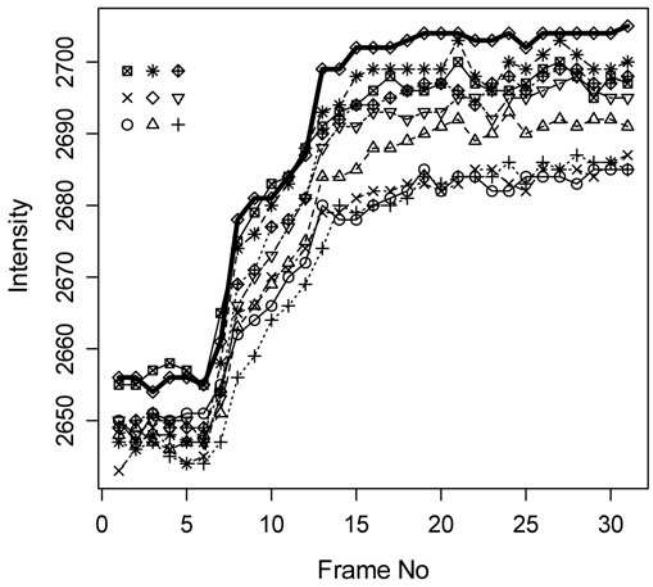

Figure 2. Intensity of pixels as a function of time (frame number) in a grid of $3 \times 3 = 9$ pixels approximately centered on a crack signal in Movie 02. Different symbols and line types represent different locations around the crack signal, which is illustrated in the NW corner of the plot.

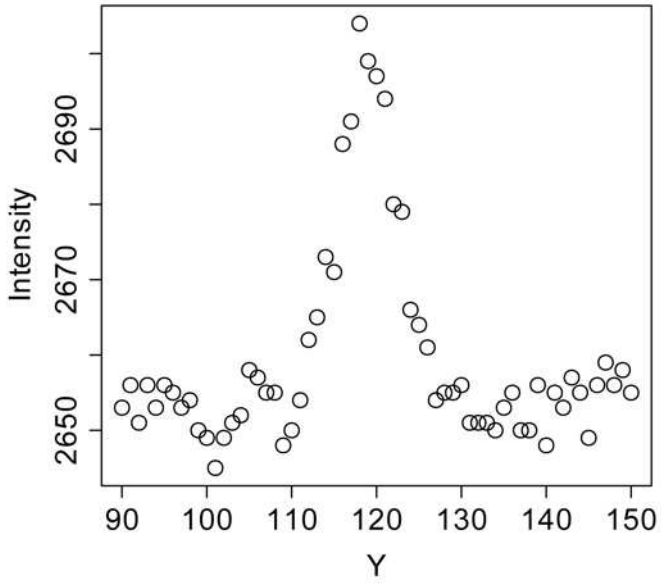

Figure 3. The intensity of pixels in Movie 02 around the crack signal center in Y direction of frame 30. A similar pattern exists in the X direction.

2.2. Noise Behavior

Figures 4 and 5 illustrate the spatial and temporal characteristics of noise in the movies and the effectiveness of subtracting out the background. Figure 4 shows the average intensity (averaging over all 256×256 pixels) versus frame number (the first row of the plots), average

intensity (averaging over all frames) versus the x coordinate (the second row of the plots) and the average intensity versus the y coordinate (the third row of the plots) of Movie 08, a movie for a specimen that does not have a crack. The three plots on the left-hand side reflect the raw data. The three plots on the right-hand side reflect the data after subtracting out the background (taken to be frame 3). As a contrast, Figure 5 contains similar plots for Movie 02, which has a strong crack signal.

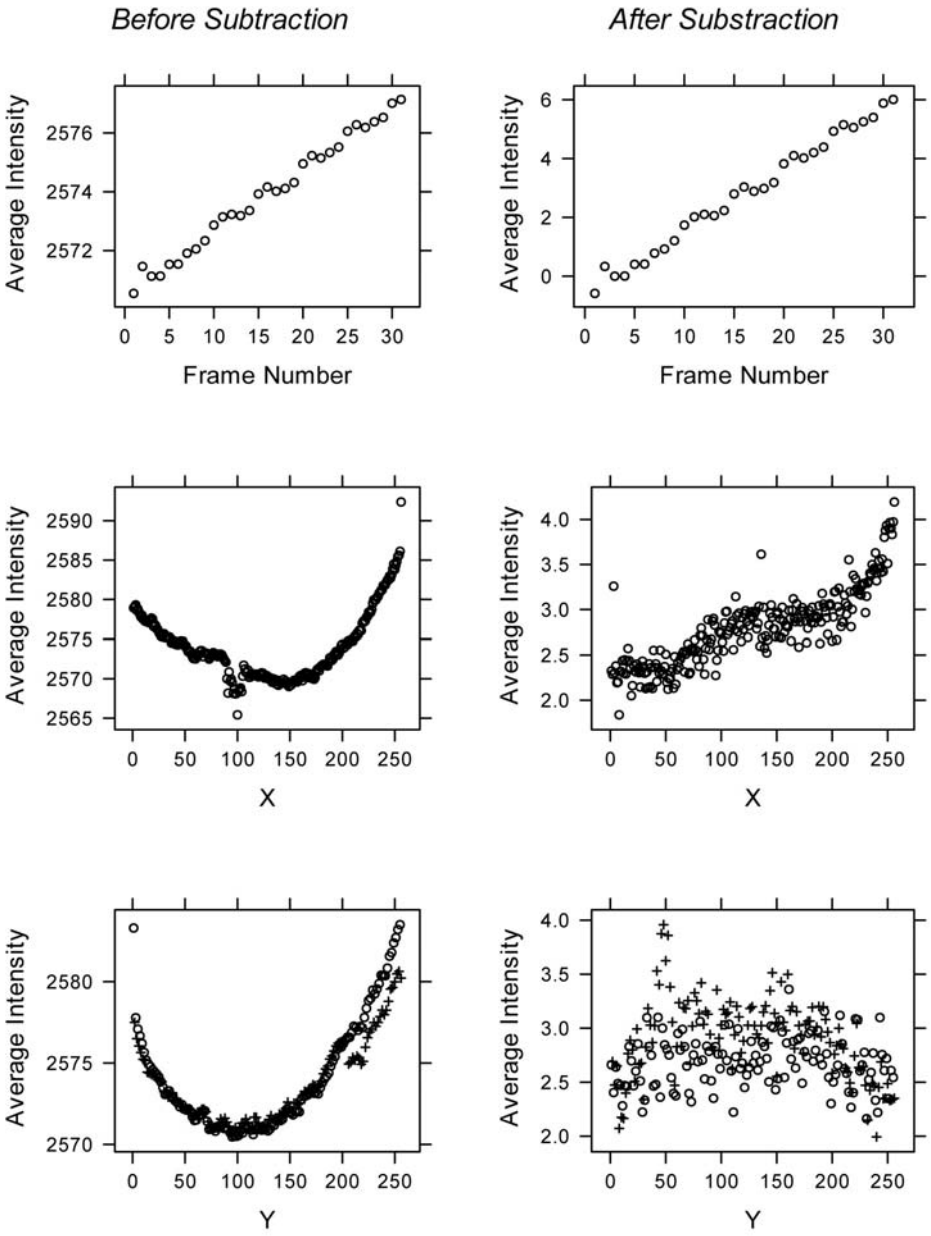

Figure 4. Average intensity by frame (first row), x coordinate (second row) and y coordinate (third row) of Movie 08 (does not have a crack). The left-hand column shows plots for the original data and the right-hand column shows plots from data after subtracting the third frame. In the two plots on the third row, the symbol "o" represents odd y values and "+" represents even y values to show the different trend of average intensity for odd and even y.

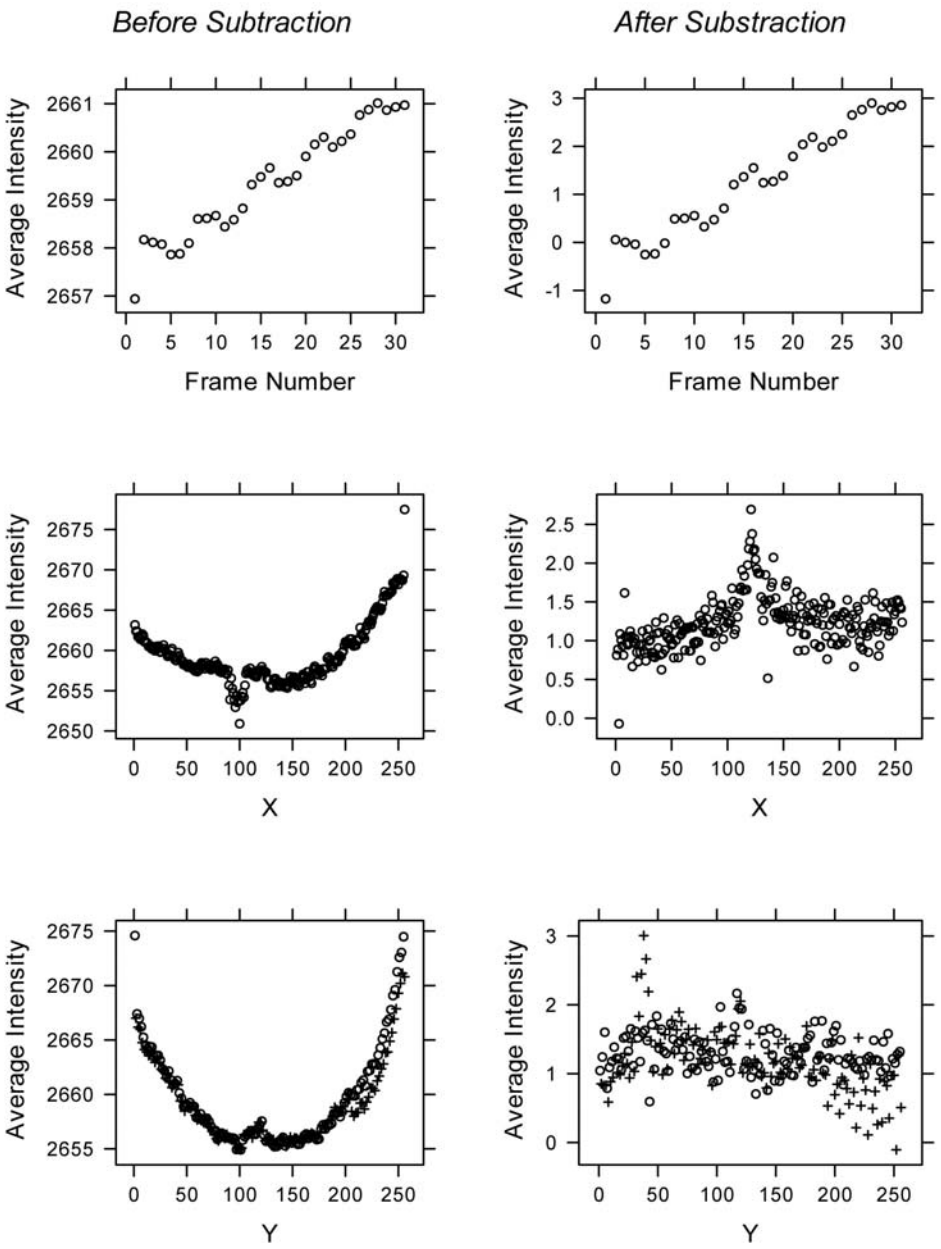

Figure 5. Average intensity by frame (first row), x coordinate (second row) and y coordinate (third row) of Movie 02 with a crack (has a crack near the center). The left-hand column shows plots for the original data and the right-hand column is the same data, after sub-tracting the third frame, in the two plots of the third row, the symbol "o" represents odd y values and "+" represents even y values to show the different trend of average intensity for odd and even y.

2.2.1. Temporal Structure of Noise

Trends and/or periodicity are clearly shown in the Figures 4 and 5. Similar trends and periodicities appear in the other movies. The temporal trends seen, for example, in Figure 4 appear throughout the image and are not driven by a crack signal and thus are a type of noise.

The exact causes of these trends and periodicities are unknown. These noises could hide the temporal signature of a real crack.

2.2.2. Spatial Structure of Noise

A U-shaped pattern appears in both the intensity versus x and intensity versus y plots as shown in the middle and bottom left-hand side of both Figures 4 and 5. Indeed, the before-subtraction plots on the left in intensity versus y plots as shown in the middle and bottom left-hand side of both Figures 4 and 5 are very similar. This similarity is due to spatial noises that are inherent in the camera and the setup that are eliminated by subtracting out the background. In the intensity versus y plot, there is a valley around $x = 100$ in all of the movies. This behavior can be easily identified by visually observing movies. A slightly brighter band appears around $x = 100$ for all four frames in Figure 1. A similar pattern appears in all of the 70 movies. Another interesting feature of the intensity appears in the third rows of Figures 4 and 5. These figures show that the odd number y pixels (represented by the symbol "o") are clearly different from the even number y pixels (represented by the symbol "+"), especially for y is greater than 200. This feature also appears in the other movies. As shown in the plots on the right-hand side of Figures 4 and 5, the underlying trends can be removed by subtracting out an early, representative frame. We use frame 3 for this purpose (the energy was not applied until after frame 3 was acquired).

Compared with Figure 4, Figure 5 shows similar patterns: periodicity and a U-shaped trend. The peaks that appear in the plots in Figure 5 in the second and third rows after subtracting frame 3 (around $x = 118$, $y = 121$, respectively) are caused by the crack signal.

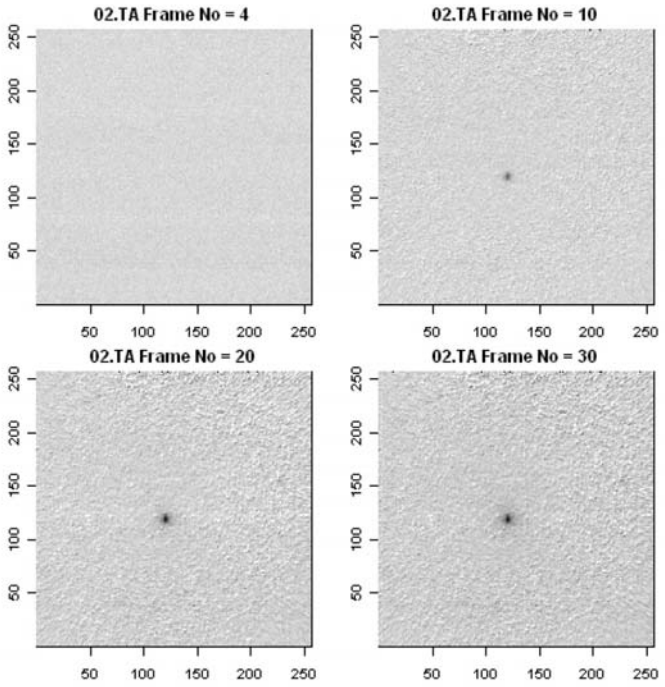

Figure 6. Frames (4, 10, 20, 30) from Movie 02 after subtracting out the 3rd frame.

2.2.3. Removing the Spatial Structure of Noise by subtracting the Frame 3

The three plots in the right-hand column of Figures 4 and 5 are the mean of intensity versus frame number t, versus position x and versus position y, respectively, after

subtraction of the background. Figure 6 shows four frames from Movie 02 after subtraction of the background. The brighter band around $x = 100$ disappeared and the image became more homogeneous when compared with the original data in Figure 1.

2.2.4. Image Shifting

Image shifting happens in some of the movies. In such movies, the structure of the frame shifts in a certain manner slowly though the whole movie. Several frames from Movie 10 are shown in Figure 7. The cloud of noisy pixels around $(x = 220, y = 180)$ is shifting in the southwest direction by two to three pixels from beginning to the end of the movie.

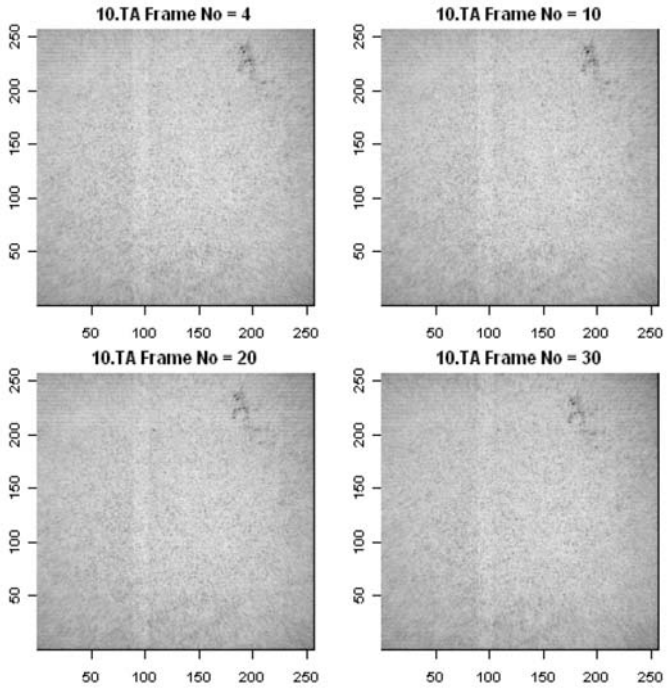

Figure 7. Frames (4, 10, 20, 30) from Movie 10. The cloud around $(x = 220, y = 180)$ shifting toward the southwest direction.

3. Signal Model

3.1. Local Signal Model

If we consider that the crack signal appears within a small region around the crack, a polynomial response surface model with up to the square terms of r and t such as

$$S = \beta_0 + \beta_1 t + \beta_2 t^2 + \beta_3 r + \beta_4 r^2 + \beta_5 tr + \beta_6 tr^2 + \beta_7 t^2 r + \varepsilon. \quad (1)$$

can be used to describe, approximately, the crack signature. Here

- r denotes the distance from the center of the crack to the pixel:

$$r = \sqrt{(x - x_c)^2 + (y - y_c)^2}.$$

- t denotes the frame number. Because the frames in the movie are collected at a constant rate, t will be proportional to the time that the frame was acquired.

- The βs are the regression coefficients that will be estimated from the data.
- ε is the residual deviation for the model.

In searching for a crack signal, the model (1) is fitted on spatial windows within the movie. The windows are circular and moved systematically across the image. By systematically moving the center point of the circle around the movie, all of the pixels in a movie will be covered at least once. The first three frames of the movie data are discarded because we subtract off the third frame as discussed in Section 2.2. The circle that is moved around has 149 pixels in each frame. The X matrix of $n = 149 \times 28 = 4172$ rows has the form of

$$\begin{pmatrix} 1 & r_1 & t_1 & r_1^2 & t_1^2 & r_1 t_1 & r_1 t_1^2 & r_1^2 t_1 \\ 1 & r_2 & t_2 & r_2^2 & t_2^2 & r_2 t_2 & r_2 t_2^2 & r_2^2 t_2 \\ . & . & . & . & . & . & . & . \\ 1 & r_n & t_n & r_n^2 & t_n^2 & r_n t_n & r_n t_n^2 & r_n^2 t_n \end{pmatrix}. \tag{2}$$

The corresponding S vector has 4172 values. The S vector and X matrix are fitted into regression model (1). There are total $(256 - 2 \times 7)^2 = 58564$ regression models for each movie. Significant differences are expected to exist in the estimates of the βs between a region with a crack signal and a region with only background noise. The estimates of the βs could be used to decide whether a crack signal exists or not. In model (1), a total 8 β estimates would be calculated for each spatial window location. It is, however, difficult to set a detection rule for such a large number of dimensions. A criterion having one or two dimensions is desired for the detection rule. We use principal components as a dimension reduction method for this purpose.

3.2. Dimension Reduction

Principal components analysis (PCA) is often used as a dimension reduction method. PCA, is described, for example, by Hastie *et al.* [1]. PCA has found applications in fields such as face recognition and image compression, and is a common technique for finding patterns in high dimension data. It is concerned with explaining the variance-covariance structure of the data through a few linear combinations of the original explanatory variables. Its general objectives are data summarization through dimension reduction and interpretation.

3.3. Principal Components Regression Model

The principal components regression model based on equation (1) is:

$$S = \theta_0 + \theta_1 \mathrm{PC}_1 + \theta_2 \mathrm{PC}_2 + \theta_3 \mathrm{PC}_3 + \theta_4 \mathrm{PC}_4 + \theta_5 \mathrm{PC}_5 + \theta_6 \mathrm{PC}_6 + \theta_7 \mathrm{PC}_7 + \varepsilon. \tag{3}$$

The variables $PC_i (i = 1, \ldots, 7)$ denote the principal components calculated from the X matrix (2) of variables used in the regression of model (1). The new PC X matrix has the form

$$\begin{pmatrix} 1 & \mathrm{PC1}_1 & \mathrm{PC2}_1 & \mathrm{PC3}_1 & \mathrm{PC4}_1 & \mathrm{PC5}_1 & \mathrm{PC6}_1 & \mathrm{PC7}_1 \\ 1 & \mathrm{PC1}_2 & \mathrm{PC2}_2 & \mathrm{PC3}_2 & \mathrm{PC4}_2 & \mathrm{PC5}_2 & \mathrm{PC6}_2 & \mathrm{PC7}_2 \\ . & . & . & . & . & . & . & . \\ 1 & \mathrm{PC1}_n & \mathrm{PC2}_n & \mathrm{PC3}_n & \mathrm{PC4}_n & \mathrm{PC5}_n & \mathrm{PC6}_n & \mathrm{PC7}_n \end{pmatrix}, \tag{4}$$

where, again, $n = 149 \times 28 = 4172$. Again, we use a model-fitting procedure similar to that used in Section 3 with a moving circle window. The moving circle has 149 pixels in each of the 28 frames (the first three frames are omitted).

For each circle position, the coefficients $\theta_i (i = 1,...,7)$ are estimated using ordinary least squares. The R function "prcomp" was used to calculate the principal components. The calculation is done by a singular value decomposition of the data matrix, rather than by using the eigenvalues of the covariance matrix. This is generally the preferred method for numerical accuracy. The estimates of θ_i are used in the following analysis to define crack-detection rules.

3.4. Principal Components Regression Results

Figure 8 shows the coefficient estimates of the first principal components for Movie 02. The three plots are three different views of the same result from different angles. The plot in the north-west corner is looking from the top. The darker the color, the larger the value of the coefficients. The plots in the south-west and north-east are looking from the X and Y directions, respectively. The three plots in the figure indicate a positive peak around $(x = 118, y = 121)$. Other movies with a crack signal show similar patterns. This indicates the coefficient for the first principal is a good indicator of crack signals. The second principal component provided no additional information for crack detection.

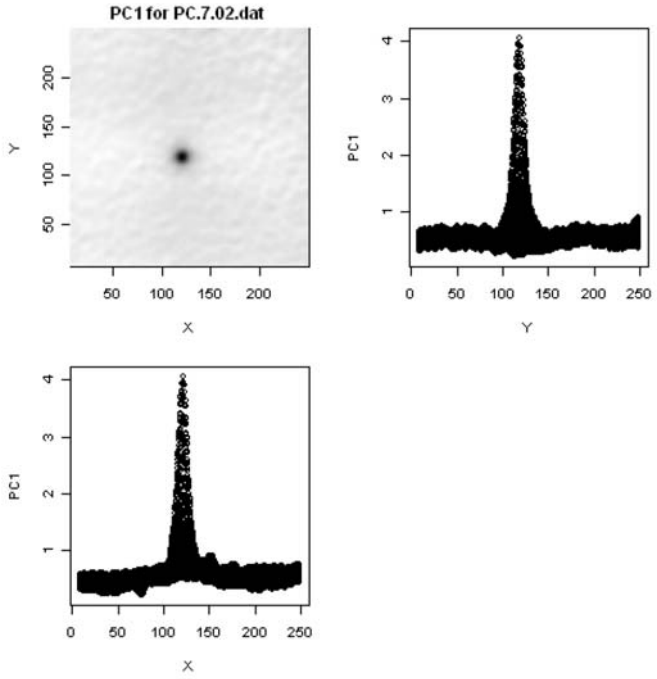

Figure 8. The estimated coefficients $(\theta_{1ij};\ i = 1, n_x;\ j = 1, n_y)$ for the first principal compo-nent (PC1) of Movie 02, viewed from three different directions. The plot in the north-west corner is looking from the top. The darker the color, the larger the value of the coefficients. The plots in the south-west and north-east are looking from the X and Y directions, respectively. Movie 02 has a strong crack signal near the center.

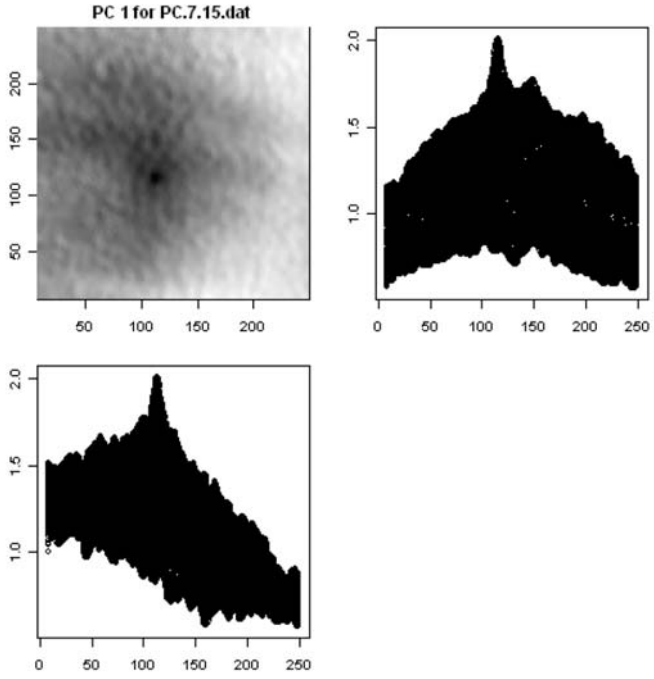

Figure 9. The coefficient estimates for the first principal component (PC1) of Movie 15, viewed from three different directions. The plot in the north-west corner is looking from the top. The darker the color, the larger the value of the coefficients. The plots in the south-west and north-east are looking from the X and Y directions, respectively. Movie 15 has a weak crack signal near the center of the frame square.

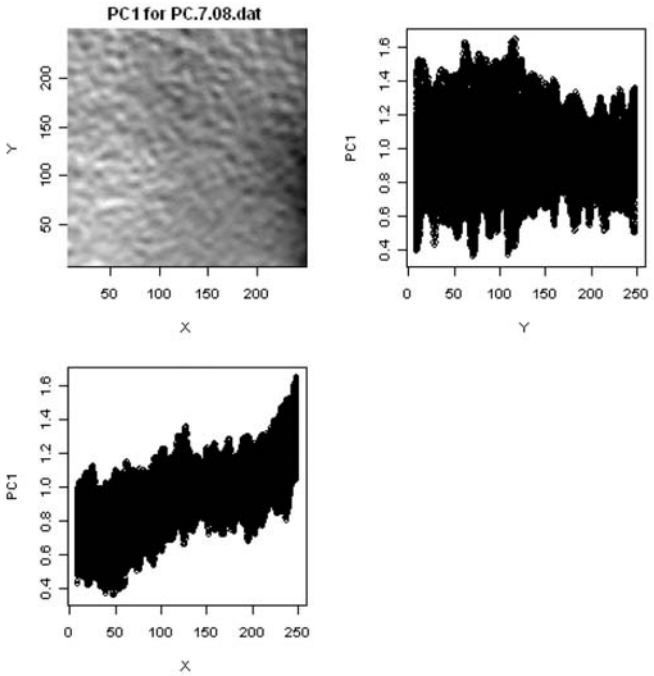

Figure 10. The estimated coefficients for the first principal component (PC1) of Movie 08, viewed from three different directions. The plot in the north-west corner is looking from the top. The darker the color, the larger the value of the coefficients. The plots in the south-west and north-east are looking from the X and Y directions, respectively. The specimen used to make Movie 08 does not have a crack.

Figure 9 shows similar plots for Movie 15. Movie 15 has a weak crack signal around the center. Comparing with the strong signals in Figure 8, the peak has much less contrast with background noise. Figure 10 shows similar plots for Movie 08, which does not have a crack. No peaks stand out in the three plots.

4. Comparison of Movies with and Without Cracks

4.1. Robust Fitting and Simple Studentized Residuals for PC1

The figures and descriptions in the Section 3 already show that the coefficient for the first principal component is a good candidate from which a decision rule can be made. However, large differences among similar plots for movies containing a signal make it hard to find a consistent detection rule using the row θ_1. In order to make the characteristic of a crack signal easier to identify, a robust fitting is performed on the θ_1 estimates and the corresponding studentized residuals are calculated as described in Huber [4] and Maronna *et al.* [8]. The reasons for using the robust regression are as follows:

- Under the usual regression model assumptions with contamination (in our case from a signal), the studentized residuals coming out of a robust regression follow approximately a standard normal distribution with 0 mean and standard deviation 1. This commonality will make the results from different movies comparable. Groups of larger residuals indicate possible crack signals.
- We choose robust regression instead of ordinary least squares (OLS) because we are trying to identify outliers. The outliers will have a large impact on the result of an OLS regression and tend to hide themselves by dragging the response surface toward them. A robust regression will put less weight on outliers and that will make the outliers stand out, which is the result we are looking for.

The residuals are used to find outliers and outliers tend to indicate the existence of a crack signal. The robust regression model is:

$$\theta_1 = \alpha_0 + \alpha_1 x + \alpha_2 y + \alpha_3 x^2 + \alpha_4 y^2 + \alpha_5 x^3 + \alpha_6 y^3 + \alpha_7 xy + \alpha_8 xy^2 + \alpha_9 x^2 y + \varepsilon. \qquad (5)$$

Here θ_1 is the coefficient of the first principal components in model (3) and x and y are the coordinates. The estimates of the coefficients of the first principal component includes $(256-2\times 7)^2 = 58564$ rows. Each row has values of x_k, y_k and θ_{1k}. The θ_{1k} denotes the coefficient of first principal component of k-th circle centered at x_k and y_k. These 56584 rows of data are used to fit model (5). The studentized residuals that result from the model fitting are used for crack detection.

Figure 11 shows the calculation result for Movie 02 (a strong signal movie). The plots in the north-west, north-east, and south-west corners show the studentized residuals from three different angles, from the top, from the x direction, and from the y direction, respectively. The plot in the south-east corner shows the hills with the maximum studentized residual (MSR) value. A clear peak exists in the plots and the peak MSR value is 46.26. Figure 12 shows a similar result from Movie 15 (a weak crack signal movie) and which results in an MSR value of 6.98 (which is much smaller than the MSR value in Figure 11). Figure 13 shows the similar results for Movie 08 (no-crack movie). No clear peak can be seen in the plot and all of the data in the image can be considered to be noise.

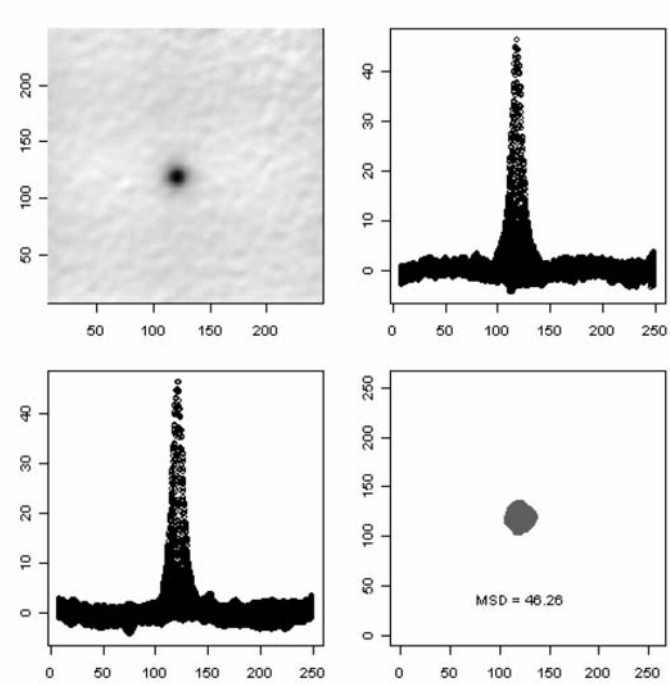

Figure 11. Robust studentized residuals for the coefficients of PC1 in Movie 02. The plot in the north-west corner is looking from the top. The darker the color, the larger the value of the coefficients. The plots in the south-west and north-east are looking from the Y directions, respectively. The plot in the south-east is looking from the top and only values larger than 5 are plotted. Movie 02 has a strong crack signal near the center. The peak MSR value on the hill is 46.26.

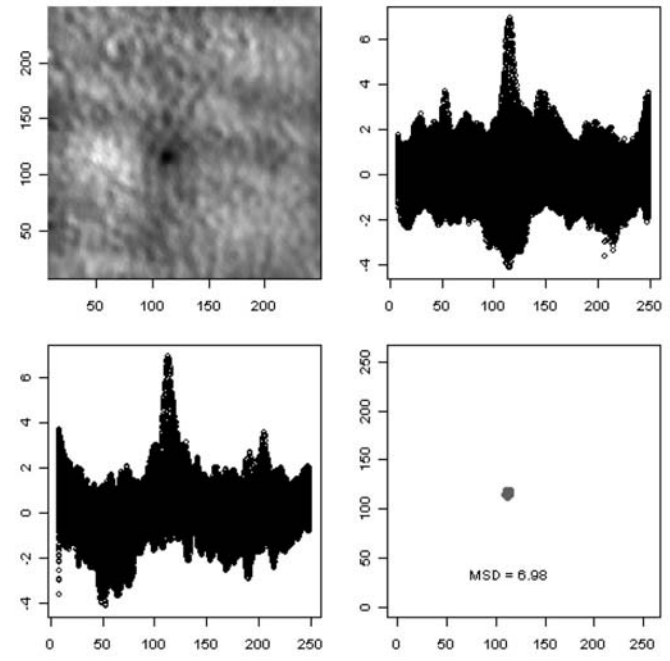

Figure 12. Robust studentized residuals for the coefficients of PC1 in Movie 15. Movie 15 has a weak crack signal near the center. The peak MSR value on the hill is 6.98.

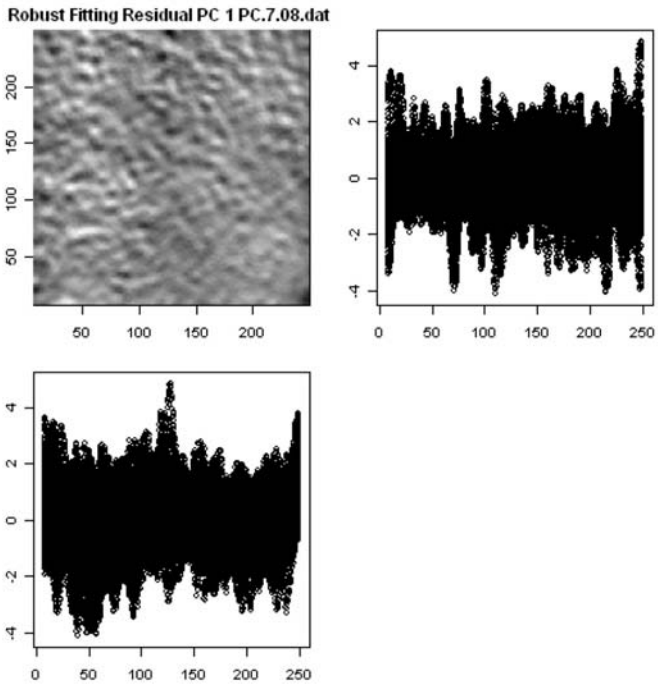

Figure 13. Robust studentized residuals for the coefficients of PC1 in Movie 08. Movie 08 was taken on a specimen that does not have a crack. The peak MSR values is 4.79.

5. Crack Detection Procedure Based on Cluster Analysis

MSR results from previous sections show that a group of large MSR values tends to form what we call a hill around the center of a crack. Such a hill will be a good indicator of a crack. Cracks, however, are not the only source of hills. A shifting image's MSR values will form a hill in its pathway, as shown in Figure 14. Figure 14 shows the result for Movie 09, which contains a weak crack signal near the center and a shifting dot at the northeast corner. The shifting dot caused the calculated MSR values formed a large hill in its pathway along with a valley (a group of extremely negative MSR values) in vicinity. One difficulty in finding the crack signals is the need to distinguish a crack signal from a shifting dot, both of which have a positive hill in the MSR plot. Real crack signals in the data generate only a positive hill. Thus a negative valley is a sign that the positive hill nearby may have been generated by a shifting dot instead of a crack signal. The task of finding a crack translates into finding a hill without a nearby valley.

5.1. Finding Hills and Valleys Using Cluster Analysis

Cluster analysis provides methods for dividing data into groups with similarities and we use cluster analysis to find hills and valleys in the studentized residuals results. The Partitioning Around Medoids (PAM) clustering algorithm (Kaufman and Rousseeuw [5]) was used to cluster the hills and valleys seen in the studentized residual plots. The algorithm will divide the observations into k groups, the points within each group will have a high degree of similarity and the observations in different groups will be as dissimilar as possible. The algorithm requires k to be specified. To identify clearly separated hills and valleys, we define k to be the smallest integer that separates the points into clusters such that all of the clusters have a diameter smaller than the distance from the nearest cluster. We start with

$k = 2$. Then we iteratively increase k until at least one of the clusters has a diameter larger than the distance from its nearest neighbor. Then $k-1$ will be the input to the PAM algorithm. If $k = 2$ and the two clusters are too close to each other at the beginning, $k = 1$ will be used in the subsequent analysis.

The detection procedure can be summarized by the following steps:

1. Mark all points which have values larger than C_{Hill}.
2. Cluster the residuals that have large values in step HillPoints into groups. These groups will be defined as hill(s).
3. Mark all points which have values smaller than C_{Valley}.
4. Cluster the points in step ValleyPoints into groups. These groups will be defined as valleys.
5. Eliminate all hills that have a valley within distance C_{Diste}.
6. Crack signals are detected if any hills are remaining. The centers of the hills will indicate the location of the centers of the crack. We will say no crack signal detected if there are no hill left.

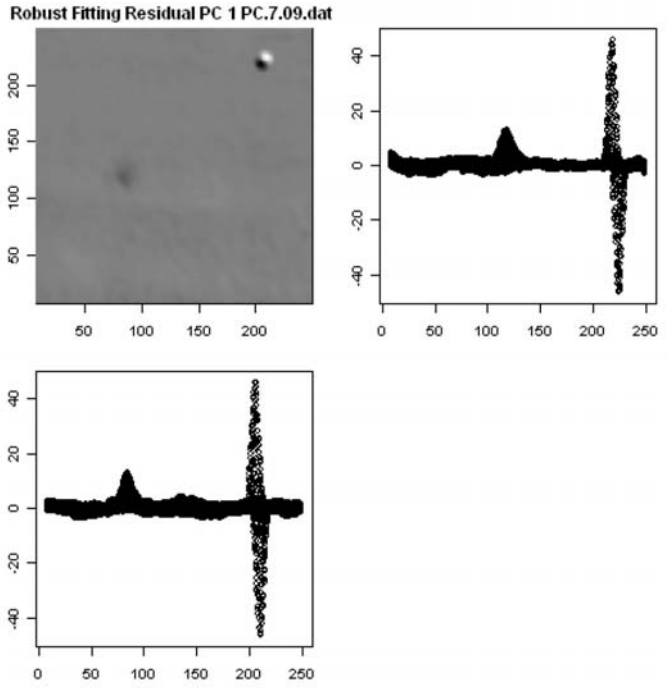

Figure 14. Robust studentized residuals for the coefficients of PC1 in Movie 09. Movie 09 has a weak crack signal near the center and a strong noise signal in the north-east corner.

5.2. Detection Thresholds

The threshold values for the above procedure are defined as:

1. C_{Hill}: The minimum value for a residual to be included in a hill.
2. C_{Valley}: The maximum value for a residual to be included in a valley.

3. C_{Dist}: The smallest distance between the hill and its nearest valley such that it still can be considered to be a crack signal.

These threshold values can be obtained by analyzing the distribution of MSR values in blank movies.

The distribution of MSR for blank movies is needed to choose the value of C_{Hill}. We obtain this distribution in the following way:

- For a movie without a crack signal, we use the maximum value of all of the studentized residuals.
- For a movie with a crack signal, the studentized residuals around the crack signal are eliminated. The maximum value of the rest of the studentized residuals will provide an MSR value. Thus each movie provides noise MSR values that will be used in the following steps

The 70 noise MSR values were extracted from the 70 movies. Figure 15 is a normal probability plot of the 70 MSR noise values. The maximum of the 70 values is 4.89. A threshold value of 5 will be good enough to keep the false alarm rate very low. The MSR values for the movies with a crack signal in our data set are larger than 5 for all movies except Movie 28.

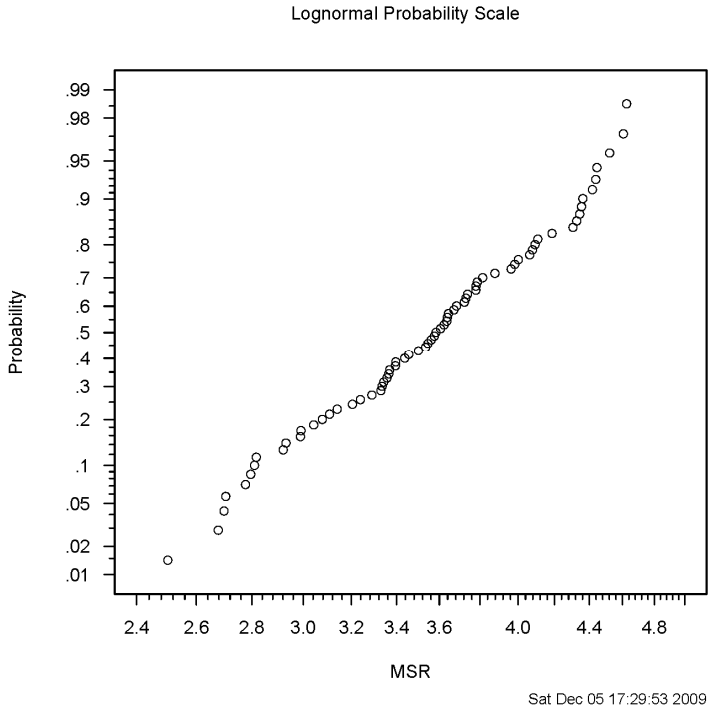

Figure 15. The lognormal probability plot of semi-MSR values from 70 movies. The maxi- mum of the 70 values is 4.89.

Based on the distribution of the signal MSR values and the distribution of the noise MSR values, we choose the following detection thresholds in order to be able to identify a hill clearly and to avoid too many false alarms:

1. $C_{\text{Hill}} = 5$ is the minimum value for a studentized residual to be included in a hill.

2. $C_{\text{Valley}} = -5$ is the maximum value for a studentized residual to be included in a valley. The value is chosen for the same reason as that for choosing C_{Hill}.

3. $C_{\text{Dist}} = 20$ pixels is the smallest distance between the hill and its nearest valley for the hill to be considered as a crack signal. A typical crack size is around 15 pixels in diameter. A hill that is fewer than 20 pixels away from a valley is probably caused by a shifting dot instead of a real crack.

5.3. Probability of Detection

The above procedure will generate a MSR value for each movie. The crack lengths of all movies were provided in the original data set. Figure 16 shows the plot of log (MSR) versus log(crack length). The linear relationship and the equal variance assumption provides a good description of the data.

The data in Figure 16 were fitted by a left-censored linear regression model. Left-censored observations arose because the MSR values for some movies taken on specimens that have a crack signal below the noise floor. The model can be expressed as

$$\log(\text{MSR}) = \mu_{\log(\text{MSR})} + \varepsilon = \alpha_0 + \alpha_1 \log(L) + \varepsilon,$$

where ε has a normal distribution with standard deviation σ. The parameter estimates are $\hat{\alpha}_1 = 2.81$, $\hat{\alpha}_0 = 13.06$ and $\hat{\alpha} = 0.67$.

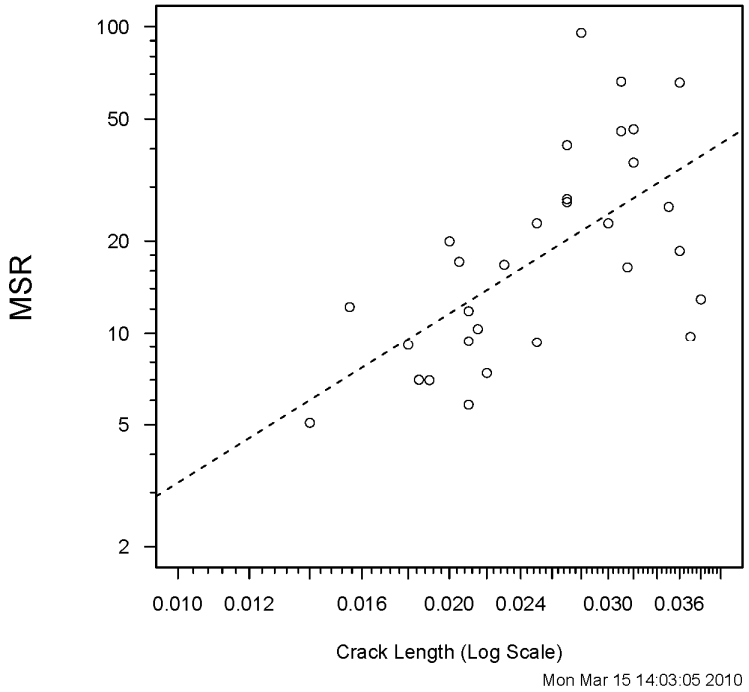

Figure 16. MSR versus crack length plot.

The probability of detection (POD) is defined as the probability of having an MSR larger than the threshold. For a specific value of crack length L, the POD can be expressed as the follows:

$$\mathrm{POD}(L) = \Pr(\mathrm{MSR} > \mathrm{MSR}_T) = 1 - \Phi_N\left(\frac{\log(\mathrm{MSR}_T) - \mu_{\log(\mathrm{MSR})}(L)}{\sigma}\right).$$

This POD function can be estimated by substituting the parameter estimates into the formula. The POD estimate versus crack length is plotted in Figure 17. The logistic regression hit/miss fitting of POD from expert-evaluation data is also plotted as the dotted line as comparison. The improvement of POD for smaller crack sizes is seen clearly in the plot. A lower confidence bound on POD could be calculated by using either the delta method or likelihood methods.

6. Conclusion and Areas for Future Research

This study has presented a statistical method for crack detection using vibrothermography data. Principal components analysis is used for dimension reduction in the data processing and robust regression and cluster analysis are used to setup the detection rule. The final detection rule gives results that are better than the expert (human) detection using visual inspection of the movie after some simple signal processing. In particular, our algorithm detected cracks in movies 7, 57 and 60 that were not identified by the expert inspectors. The POD curve calculated from the distribution of the MSR has a better POD estimate for small cracks.

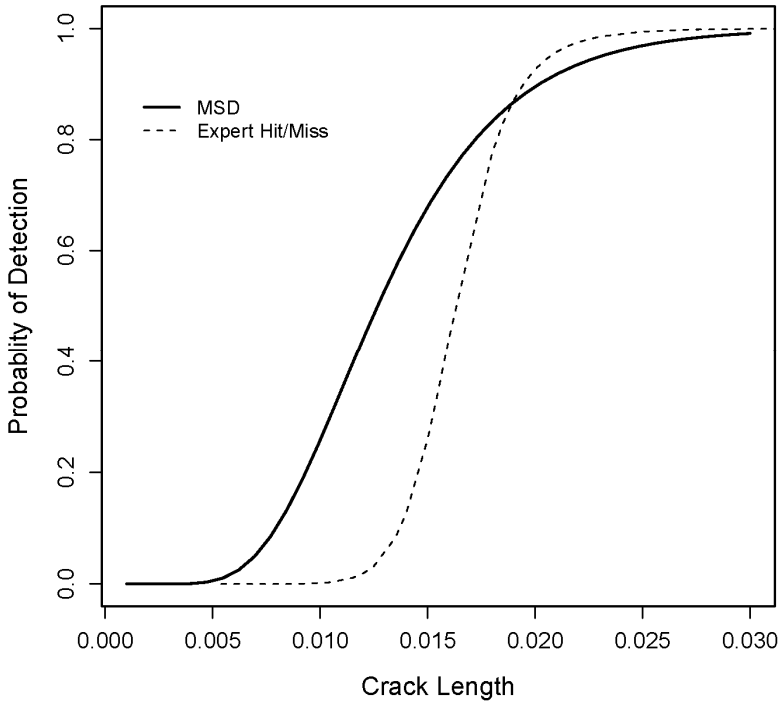

Figure 17. Probability of detection versus crack length plot.

Possible future research directions of this research include:

- Vibrothermography tends to be a noisy inspection method. As we have seen, some noises can be eliminated by simple image processing methods like subtracting out the background. Current research (at Iowa State University and elsewhere) seeks finds

additional ways to do increase the vibrothermography inspection signal-to-noise ratio. For example Li *et al.* [7] describe the results of a multi-site experiment to study repeatability and reproducibility among different vibrothermography inspection systems.

- To help the effort to improve vibrothermography inspection, part of current research effort at Iowa State University is to obtain a better understanding of the physical theory behind vibrothermography and the relationship between vibration and heating (e.g., Renshaw *et al.* [10]).
- The measurement of the data used in this study stops before the temperature begins to fall. Vibrothermography data in the future should include the data after the samples begin to cool down. These more complete data should increase the power of the detection and lower the false alarm rate.
- Improved crack detection methods would also be more sensitive and accurate if the various noises (e.g., trend, periodicity, and image shifting) could be eliminated or reduced by improving the inspection system.
- A simulation study (simulating more movies) would provide more insight into the principal components analysis of the movies and be used to explore possible directions to improve the detection algorithm.
- If more than one crack is present, our algorithm has the potential to detect both of them. On such a case there will be two peaks in the plots of the PC1 coefficients. Interesting questions then arise about the importance (e.g., from a safety point of view) of two cracks versus one larger crack.
- Our detection method used a combination of model fitting within a moving window to capture the crack signature and PCA to summarize the results, leading to a detection algorithm. There are, of course, other possible approaches. For example, as suggested by one of the reviewers, one might also use a generalization of an EWMA detection scheme to the spatial-temporal domain. In another approach, Li *et al.* [6] use the concept of a matched filter to account for the crack signature before applying a detection rule based on a signal-to-noise ratio.

Acknowledgments

This material used in the paper is based upon work supported by the Air Force Research Laboratory under Contract # FA8650-04-C-5228 at Iowa State University's Center for NDE. The data in this paper were generated at the Pratt and Whitney Aircraft Engine Company under NASA TEST Contract # NAS3-98005 as part of Task Order # 21 "Development and Integration of Inspection Technology for Damage Detection in On-wing Engine Configurations."

References

1. Hastie, T., Tibshirani, R. and Friedman, J. (2009). *The Elements of Statistical Learning, 2nd Edition: Data Mining, Inference, and Prediction*, 2nd edition. Springer Series in Statistics, Springer New York.
2. Henneke, E. G. and Jones, T. S. (1979). Detection of damage in composite materials by vibrothermography. *ASTM Special Technical Publication*, 696, 83-95.
3. Holland, S. D. (2007). First Measurements from a New Broadband Vibrothermography Measurement System. In D. O. Thompson and D. E. Chimenti (Eds.), *Review of*

Progress in Quantitative Nondestructive Evaluation, Volume 894 of *American Institute of Physics Conference Series*, 478-483.

4. Huber, P. J. (2009). *Robust Statistics*, 2nd edition. Wiley-Interscience.
5. Kaufman, L. and Rousseeuw, P. J. (1990). *Finding Groups in Data: An Introduction to Cluster Analysis*. Wiley-Interscience.
6. Li, M., Holland, S. D. and Meeker, W. Q. (2010). Statistical methods for automatic crack detection based on vibrothermography sequence-of-images data. *Applied Stochastic Models in Business and Industry*, 26, 481-495.
7. Li, M., Holland, S. D. and Meeker, W. Q. (2011). Quantitative multi-inspection-site comparison of probability of detection for vibrothermography nondestructive evaluation data. *To appear in Journal of Nondestructive Evaluation*, 30, 172-178.
8. Maronna, R. A., Martin, D. R. and Yohai, V. J. (2006). *Robust Statistics: Theory and Methods*. Wiley.
9. Reifsnider, K. L., Henneke, E. G. and Stinchcomb, W. W. (1980). *Mechanics of Nonde-structive Testing: Conference on the Mechanics of Nondestructive Testing*. Plenum Press.
10. Renshaw, J., Holland, S. D. and Thompson, R. B. (2008). Measurement of crack opening stresses and crack closure stress profiles from heat generation in vibrating cracks. *Applied Physics Letters*, 93, 081914.

Authors' Biographies:

Chunwang Gao earned a B.S. in Physics from Peking University in 1998. He received MS degrees in Physics (2004), Statistics (2005) and Computer Engineering (2009) from Iowa State University. He received a PhD degree in Statistics in 2010, also from Iowa State University. He is currently a private consultant living in the Richman VA area.

William Q. Meeker is a Professor of Statistics and Distinguished Professor of Liberal Arts and Sciences at Iowa State University. His interests are in the areas of reliability data analysis, statistical methods for quality improvement, statistical planning and inference, and statistical computing. He is a Fellow of the American Statistical Association and an elected member of the International Statistics Institute. Dr. Meeker is a former editor of *Technometrics*. He is the co-author of two books, five book chapters, and of numerous publications in the engineering and statistical literature.